

Absorption and Emission Spectroscopy of Benzene in Cryogenic Solutions. An Estimate of the Intermolecular Potential

F. Li, J. Lee, and E. R. Bernstein*

Department of Chemistry, Colorado State University, Fort Collins, Colorado 80523 (Received: March 5, 1982;
In Final Form: May 11, 1982)

Absorption and emission spectra for C_6D_6 in CH_4 , C_2H_6 , C_2H_4 , C_3H_8 , C_3H_6 , C_4H_8 , and NF_3 between ~ 90 and ~ 220 K are presented and discussed in terms of intermolecular interactions in the liquid state. These cryogenic liquid solutions are chosen because sharp, well-defined spectroscopic features for benzene can be discerned in these relatively simple systems. Gas-to-liquid shifts for both emission and absorption are characterized; the differences between the two are related to intermolecular Franck-Condon shifts. The absorption line width is found to be constant as the temperature is increased while the emission line width broadens to the low-energy side as temperature is increased. A series of apparently reasonable assumptions can be made which subsequently allows one to obtain a shape for the intermolecular repulsive potential for ground-state benzene solute/hydrocarbon solvent. The repulsive part of the potential function near the equilibrium position closely approximates a harmonic oscillator. If the potential were symmetrical about its equilibrium position, which of course, it is not, an intermolecular force constant of 3.4×10^{-2} mdyn/Å and a "phonon" frequency of 8×10^{12} s $^{-1}$ (~ 250 cm $^{-1}$) would result.

Introduction

While the liquid state occupies only a small portion of the temperature-pressure phase diagram, it is probably the most important phase in terms of practical matters and experience. Nonetheless, unlike the situation for solids and gases, relatively few detailed high-resolution spectroscopic studies have been reported for liquids; linewidths and congestion problems seem to have discouraged or foiled most attempts. We have demonstrated, however, that low-temperature liquids (i.e., N_2 , O_2 , CO , NF_3 , CH_4 , C_2H_6 , etc.) are not only reasonable solvents for a number of solutes (i.e., C_6H_6 , C_4H_4 , OsO_4 , H_2CO , SO_2 , and others) but also excellent spectroscopic hosts yielding well-resolved, relatively sharp emission and absorption spectra.¹ Based on these observations, we have attempted to analyze such data as absorption and emission line widths and their temperature dependences, gas-to-liquid shifts for absorption and emission features and their temperature dependences, Franck-Condon shifts for absorption and emission features and their temperature dependences, as well as other results in terms of microscopic details of liquid structure and dynamics.

Many studies of liquids have taken place over the years,² including X-ray scattering, neutron scattering, light-scattering spectroscopy, and theoretical modeling. The difficulty in dealing with the liquid state is twofold: characteristic time and energy scales. For a gas, the scales are collision time, mean-free path time, and (potential energy/kinetic energy) $\ll 1$. Processes occurring on times shorter than collision times are in the microscopic molecular regime and processes occurring on time scales greater than the mean-free path time are in the macroscopic (continuum or hydrodynamic) regime. For the solid, the time scales and energy ratios are reversed; the potential

energy is much greater than the kinetic energy. For the liquid state, however, no such limiting conditions seem appropriate for the separation between time and energy scales. Thereby, it would be important to generate from spectroscopic data, where possible, some estimates of various parts (i.e., repulsion, attraction, dispersion, etc.) of the liquid-state intermolecular potential. In this work an estimate of the intermolecular potential for small molecule hydrocarbon liquids, as probed by the ${}^1B_{2u} \leftarrow {}^1A_{1g}$ transition of benzene, is presented. In another paper,³ some estimates of kinetics and energy dynamics behavior will be discussed for similar systems.

In the experiments reported in this communication, electronic absorption and emission spectra of the ${}^1B_{2u} \leftarrow {}^1A_{1g}$ transition of benzene are studied as a function of solvent (CH_4 , C_2H_6 , C_2H_4 , C_3H_8 , C_3H_6 , C_4H_8 , NF_3) and temperature ($90 \leq T \leq 220$ K). Probing these cryogenic liquids composed of small simple molecules with a molecule as well known and studied as benzene has enabled us to circumvent the usual problems associated with broad unstructured liquid-state spectra. Other probe or solute systems with different geometrical and electronic structure (i.e., $C_4N_2H_4$, $C_6H_5CH_3$, $C_{10}H_8$) allow different aspects of solution energetics and kinetics to be investigated.⁴

It is observed that in low-temperature hydrocarbon liquids the lifetime of the ${}^1B_{2u}$ excited state of benzene is of the order of 10^{-7} s,³ while the solvent relaxation time is of the order of 10^{-11} – 10^{-12} s. Emission from benzene in these solvents therefore originates from the excited inter- and intramolecular equilibrium configuration. This excited-state equilibrium configuration is different from the ground-state equilibrium configuration due to the difference between the interaction of the benzene ${}^1A_{1g}$ and ${}^1B_{2u}$ electronic states with the surrounding solvent molecules. Absorption, of course, originates with the ground-state equilibrium configuration. Both processes, however, end on the appropriate Franck-Condon part of the respective terminus state (a "vertical transition"). The difference

(1) (a) E. R. Bernstein and J. Lee, *J. Chem. Phys.*, **74**, 3159 (1981); (b) M. W. Schauer, J. Lee, and E. R. Bernstein, *J. Chem. Phys.*, **76**, 2773 (1982); (c) J. Lee and E. R. Bernstein, *ibid.*, submitted for publication.

(2) (a) R. D. Mountain, *Crit. Rev. Solid State Sci.*, **1**, 5 (1970); (b) A. H. Narten, *J. Chem. Phys.*, **67**, 2102 (1977); (c) H. Nomura, S. Koda, and Y. Miyahara, *Bull. Chem. Soc. Jpn.*, **52**, 3249 (1979); (d) J. P. Hansen and J. R. McDonald, "Theory of Simple Liquids", Academic Press, New York, 1976.

(3) F. Li, J. Lee, and E. R. Bernstein, *J. Phys. Chem.*, submitted for publication.

(4) F. Li, J. Lee, and E. R. Bernstein, unpublished results.

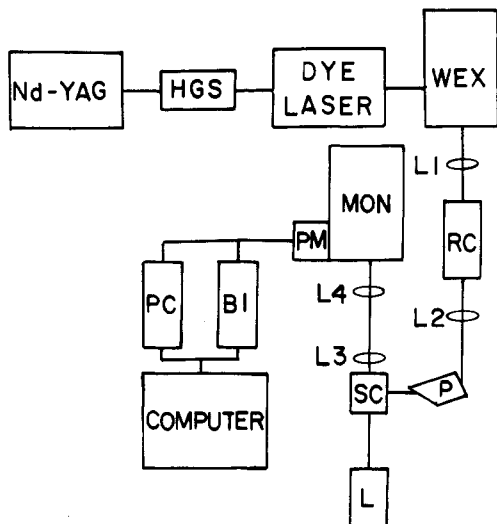


Figure 1. Experimental setup for absorption and emission: HGS, harmonic generator and separator; WEX, wavelength extender which doubles the frequency of output of dye laser; L1, L2, 50-cm focal length Suprasil lenses; P, Pellin Broca prism; SC, sample cell; L, xenon lamp for absorption experiment; L3, 1-in. focal length Suprasil collecting lens; L4, 10-cm focal length lens; RC, Raman shifter high-pressure H_2 cell (270 psi H_2); Mon, 1-m scanning monochromator; PM, photon multiplier tube RCA C31000M; PC, photon-counting system; BI, boxcar integrator.

between liquid-state emission and absorption energy for a series of similar solvents can be employed to map out parts of the ground-state intermolecular potential surface. Such data may also be useful in the elucidation of the structure of the solvent sphere or cage surrounding the probe molecule.

Specifically, this report will discuss how different solvents affect the emission and absorption spectra of the benzene- d_6 solute, why there are differences in the line broadening for absorption and emission vibronic features as a function of temperature, and how one can approximately map the repulsive part of the intermolecular potential for the ground-state benzene/small molecule hydrocarbon solvent interaction from the observed data.

Experimental Section

Samples are prepared from C_6D_6 (Aldrich Gold Label), further purified by reaction with potassium in a vacuum line and distilled through low-temperature molecular sieve, and the highest attainable commercial purity solvents. Solvents are further purified by vacuum distillation through low-temperature molecular sieve and activated charcoal, as previously detailed in ref 1. Samples are premixed in a 7-L stainless steel can; concentrations are calculated from known volumes and vapor pressure curves.

The sample cell is a 3.8-cm pathlength 15-mL volume stainless steel container with Suprasil quartz windows. It is cooled by a CT1 350 cryogenic mechanical helium refrigerator. Temperature is controlled by a diode sensor and a heater placed at the base of the cold station of the refrigerator.

For an absorption experiment, filtered xenon lamp light is passed through the liquid sample, dispersed by a 1-m monochromator with a 2400 groove/mm grating, and detected by an C3100M photomultiplier tube operated in a photon-counting mode. Emission is generated by directly exciting the ${}^1B_{2u}$ state with output from a doubled, Raman-shifted (270 psi H_2) Nd:YAG pumped rhodamine 610 dye laser. This combination produced roughly 1–2 mJ/pulse at 2650–2550 Å. A Pellin Broca prism separates the various overtones from the Raman cell. The first stimu-

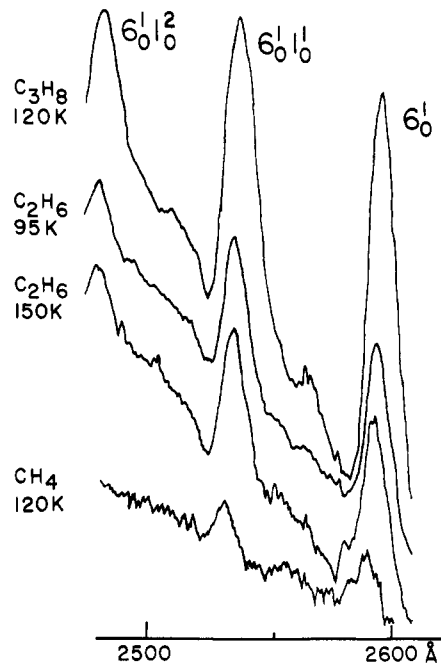


Figure 2. Absorption spectra of C_6D_6 in various solvents and at different temperatures. Also shown in C_2H_6 at two different temperatures indicating that the line width is insensitive to the temperature change.

lated anti-Stokes frequency is passed through the cell unfocused. This configuration is depicted in Figure 1. Fluorescence is dispersed and detected as indicated above for absorption. The output of the photomultiplier tube is processed by a boxcar averager (PAR 162/164). The signals from the boxcar are further analyzed by an HP 9845S desktop computer.

Results

The absorption and emission spectra of C_6H_6 and C_6D_6 are in all respects identical in each solvent used except for a constant electronic state shift and the well-known usual vibrational isotope effect. Only the C_6D_6 results are reported in this discussion as this solute was investigated more extensively due to its potential usefulness in energy-transfer experiments.

Figure 2 shows the absorption spectra of C_6D_6 in various solvents. It is also evident from this representation that the absorption line width is independent of temperature. However, Figure 3 presents data which clearly demonstrate that the situation is quite different with respect to the temperature behavior of the emission spectra of C_6D_6 in these solvents. The increase in emission line width with increasing temperature is mainly due to an unsymmetrical broadening to the low-energy side of each emission feature. This broadening occurs at the lowest concentration employed (0.3 ppm) indicating that the effect results from a change in the environment of a single solute molecule.

Exciting different vibronic bands of the ${}^1B_{2u}$ state and different parts of particular features, including the 0–0 transition, always results in an identical spectrum. Excitation at energies lower than the 0–0 transition results in no fluorescence whatsoever. It can be concluded from these data the fast intramolecular vibrational relaxation takes place to the zeroth vibrational state of ${}^1B_{2u}$ from which all emission originates. The main emission progression from this state is $6_0^1 1_n^0$ ($n = 0, 1, \dots$) with molecular Franck-Condon maximum at $n = 1$.

Tables I and II summarize these results and give emission and absorption gas-to-liquid shifts and line widths as a function of temperature.

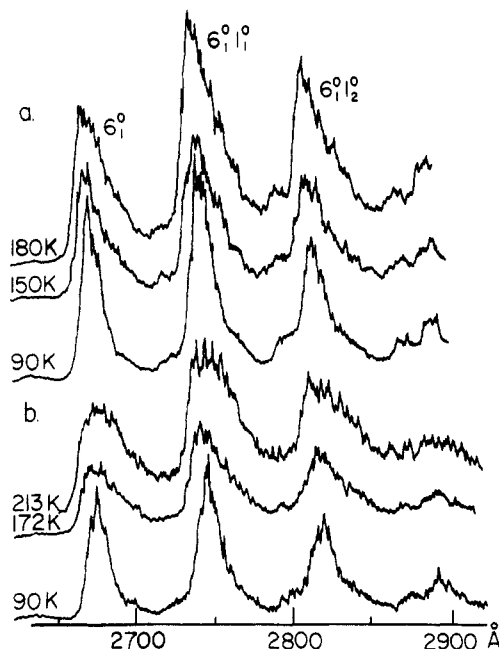


Figure 3. Fluorescence spectra of C_6D_6 in (a) C_2H_6 and (b) C_3H_8 at various temperatures. At the higher temperature the line width broadens and the broadening is mainly toward the lower energy side of the feature.

TABLE I: C_6D_6 ${}^1B_{2u} \leftarrow {}^1A_{1g}$ Transition in Various Solvents^a

	absorption		emission	
	0-0 ^b (± 20)	gas-to-liquid shift	0-0 ^c (± 20)	gas-to-liquid shift
$C_6D_6/1-C_2H_6$	37 986	-303	37 862	-427
C_6D_6/C_3H_8	38 010	279	37 891	398
C_6D_6/C_2H_4	38 036	253	37 940	349
C_6D_6/C_3H_8	38 019	270	37 950	339
C_6D_6/C_2H_6	38 042	247	37 984	305
C_6D_6/CH_4	38 112	177	38 080	209
C_6D_6/NF_3	38 236	53	38 228	61

^a Absorption 0-0, gas-to-liquid shift in absorption, and gas-to-liquid shift in emission. All energies are given in cm^{-1} . Gas-phase value of the C_6D_6 0-0 is 38 289 cm^{-1} . C. S. Parmenter, *Adv. Chem. Phys.*, **22**, 365 (1972), and this experiment. ^b Calculated from observed 6_1^0 . ^c Calculated from observed 6_1^0 .

Discussion

Electronic transitions of molecules in solution are different from those in the isolated molecule due to the presence of a "coordination sphere" or "cage" of solvent molecules surrounding the molecule of interest. According to the Franck-Condon principle, electronic transitions occur on such a short time scale that nuclei of the solute and solvent can be considered to be stationary over the time duration of the process. The configuration of the excited ${}^1B_{2u}$ and ground ${}^1A_{1g}$ solute/solvent equilibrium states are different due to the difference in the ${}^1B_{2u}$ and ${}^1A_{1g}$ solvation energies. This situation is illustrated schematically in Figure 4. One can thus regard the absorption process for benzene in solution as consisting of an electronic promotion from the ground equilibrium state (${}^1A_{1g}$ in the minimum energy solvent cage configuration for a given temperature) to the excited Franck-Condon state (${}^1B_{2u}$ in the same configuration solvent cage). Fast solvent relaxation (10^{-12} - 10^{-11} s for a diffusion constant of 10^{-5} cm^2/s) brings these excited (Franck-Condon) state systems to the excited equilibrium configuration in roughly 10^{-5} - 10^{-4} ${}^1B_{2u}$ solution lifetimes. The long lifetime of the

TABLE II: Emission Line Width of the C_6D_6 6_1^0 Transition in Various Solvents and at Different Temperatures^a

T/K	line width	diff between half-height and position max	
		higher energy	lower energy
C_6D_6/C_3H_8			
90	227	87	140
165	331	114	217
205	529	157	372
C_6D_6/C_2H_6			
90	192	70	122
150	245	105	140
180	331	114	227
C_6D_6/C_2H_4			
110	238	91	141
140	246	99	147
172	340	137	207

^a All values are given in cm^{-1} .

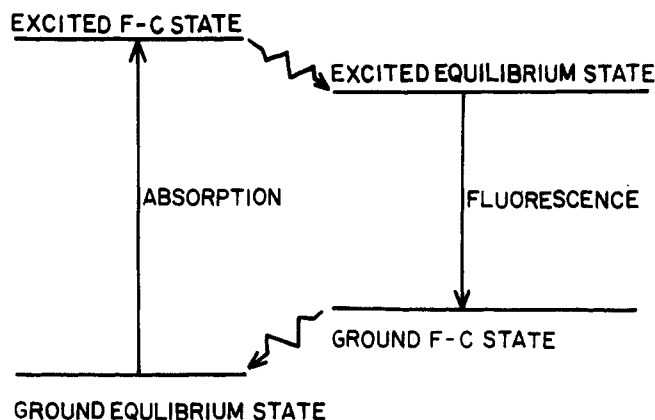


Figure 4. Ground and excited Franck-Condon and equilibrium states in the solvent. Wavy lines represent intermolecular solvent relaxation.

${}^1B_{2u}$ state³ (10^{-7} s) in these solutions thereby ensures that emission originates from the excited equilibrium configuration. In like manner the ground Franck-Condon state and not the ground equilibrium state is the final state resulting from the emission process. Subsequent solvent sphere relaxation takes place on the 10^{-12} - 10^{-11} s time scale to return the system to the ground equilibrium configuration. It is further quite likely that the intramolecular vibrational relaxation takes place on a similar time scale.

The observation that absorption line widths are temperature independent while emission line widths increase to the low-energy side with increasing temperature can be used to generate a semiquantitative estimate of the intermolecular potential in the ground configuration. Figure 5 presents a diagram which demonstrates this argument with a plot of the various potential functions with respect to an averaged intermolecular coordinate. For simplicity only the zero vibrational levels and one quantum of the ν_6 levels in each electronic state are shown. The above line width results uniquely fix the qualitative relative positions of the two intermolecular surfaces. Thus, based on a Boltzmann distribution in either ${}^1B_{2u}$ or ${}^1A_{1g}$ state prior to any radiative transitions and the Franck-Condon principle, one can obtain information on the upper surface from the absorption data and information on the lower surface from the emission data.

Since benzene is a nonpolar molecule in both electronic states, the induced dipole-induced dipole interaction between it and surrounding solvent molecules can be taken as small. Moreover, absorption and emission gas-to-liquid

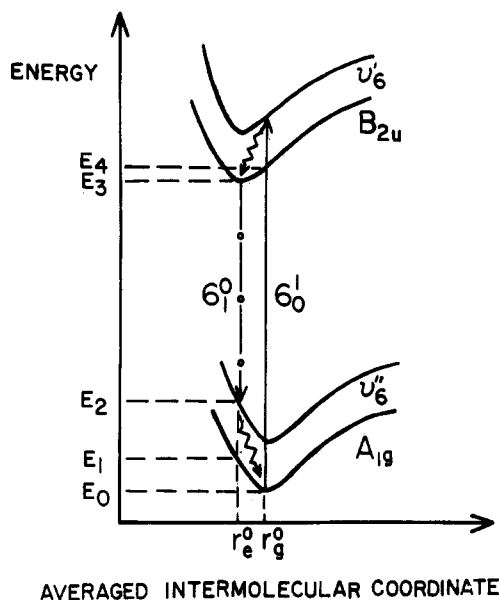


Figure 5. Potential energy diagram as a function of averaged intermolecular coordinate. For simplicity only 6_0^1 absorption (\rightarrow) and 6_0^1 emission ($0 \rightarrow 0$) are shown. (---) represents the nonradiative intramolecular vibrational and intermolecular solvent relaxation. r_g^0 is the equilibrium-averaged intermolecular coordinate for the minimum potential energy in the ground-state potential. r_e^0 is the equilibrium-averaged intermolecular coordinate for the minimum energy in the excited-state potential. It is assumed that the intermolecular potential has the same form in the ground and excited states. The only difference between them is the relative shift in position of the minimum potential point. It is further assumed that the vibrationally excited molecular state in either electronic state (i.e., A_{1g} and B_{2u}) has the same intermolecular potential function. ($E_4 - E_0$) represents the transition energy of the absorption $0 \rightarrow 0$. ($E_3 - E_1$) represents the transition energy of the emission $0 \rightarrow 0$ peak. Since it is assumed that intermolecular potential has a steep repulsive part and a smooth slowly rising long-range attractive part, one obtains $(E_1 - E_0) \gg (E_4 - E_3)$. The Franck-Condon shift thus can be simplified as $\Delta E_{FC} \approx E_1 - E_0$. Zero point energies have been omitted for simplicity in this presentation.

shifts for solvents that have no dipole moment (CH_4 , C_2H_6 , C_2H_4) and those that have a dipole moment (NF_3 , C_3H_8 , C_3H_6 , C_4H_8) seem to follow the same general trends. These changes seem best correlated with polarizabilities ($1/\rho[(n^2 - 1)/(n^2 + 2)]$ in which ρ is the density and n is the refractive index of the solvent) rather than solvent dipole moment (see Figure 6).

In the ensuing discussion we therefore make the following simplifying assumptions: (1) the intermolecular potential has the same form in the ground and excited states. The only difference between the two potentials is the relative position of the minimum potential point, that is, r_e (excited-state equilibrium position) $\neq r_g$ (ground-state equilibrium position); (2) vibrationally excited molecular states (ν_6 in particular) in either electronic state have the same intermolecular potential function as do their respective vibrationless electronic states. While this latter condition may be weakly violated for large amplitude bending modes it should be reasonable for stretching modes like ν_6 .

With these assumptions one concludes that the Franck-Condon portion of the upper potential, accessed by absorption, must be relatively flat. Likewise, from the emission spectrum one concludes that the corresponding Franck-Condon accessed portion of the ground-state potential must be quite steep. Since it is generally well established and accepted that the intermolecular potential has a steep repulsive part and a relatively flat, long-range, smooth attractive part, the minimum point for the upper surface must lie at a smaller intermolecular separation r

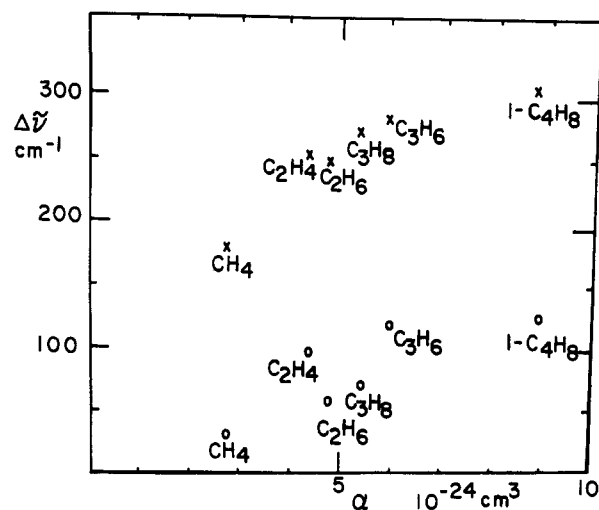


Figure 6. Plot of absorption gas-to-liquid shifts (X) and Franck-Condon shifts (O) of C_6D_6 in various solvents as a function of the polarizability of the solvents.

than the lower surface ($r_e < r_g$).

It is known⁵ that the excited ${}^1B_{2u}$ state of benzene is somewhat ($\sim 0.08 \text{ \AA}$) larger than the ${}^1A_{1g}$ ground state. Hence, benzene has a larger polarizability in the ${}^1B_{2u}$ state than in the ${}^1A_{1g}$ ground state, as its π electronic structure is more diffuse or extended. The reduction of the average equilibrium intermolecular normal coordinate from r_g to r_e is thus consistent with the expanded size and polarizability. The attractive long-range dispersion forces must therefore increase more than the repulsive forces in the excited state. Figure 5 depicts this situation for the above assumptions and conditions.

In order to place these ideas on a more quantitative footing, we turn now to a detailed quantum mechanical/macroscopic treatment of solvent effects presented by McRae.⁶ McRae has given expressions for the gas-to-liquid solvent shifts for both absorption and emission based on electrostatic interactions. Extending the calculations to second order, we can derive eq 1 and 2 for the gas-to-liquid shifts for the transitions between the i th excited state and the ground state. While McRae's paper

$\Delta \tilde{\nu}_{i0}(\text{absorption}) =$

$$\frac{1}{hc}(2.13 \times 10^{-30}) \left[\sum_{j \neq 0} \left(\frac{1}{\bar{\nu}_{j0}^2} - L_{j0} \right) \frac{f_{j0}^2}{a^3} \frac{n_{j0}^2 - 1}{2n_{j0}^2 + 1} - \sum_{j \neq i} \left(\frac{1}{\bar{\nu}_{ji}^2} - L_{ji} \right) \frac{f_{ji}^2}{a^3} \frac{n_{ji}^2 - 1}{2n_{ji}^2 + 1} \right] + \frac{1}{hc} \frac{(M_{00}^i)^2 - (M_{ii}^i)^2}{a^3} \frac{n_0^2 - 1}{2n_0^2 + 1} + \frac{2}{hc} \frac{M_{00}^i (M_{00}^i - M_{ii}^i)}{a^3} \left[\frac{D - 1}{D + 2} - \frac{n_0^2 - 1}{n_0^2 + 2} \right] + \frac{6}{hc} (M_{00}^i)^2 \frac{(\alpha_0^i - \alpha_i^i)}{a^6} \left[\frac{D - 1}{D + 2} - \frac{n_0^2 - 1}{n_0^2 + 2} \right]^2 \quad (1)$$

should be consulted for a detailed elaboration of the de-

(5) J. H. Callomon, T. M. Dunn, and I. M. Mills, *Phil. Trans. R. Soc. (London)*, Ser. A, 259, 499 (1966).

(6) (a) E. G. McRae, *J. Phys. Chem.*, 61, 562 (1957); (b) N. S. Bayliss and E. G. McRae, *ibid.*, 58, 1002 (1954); (c) See also: A. T. Amos and B. L. Burrows, *Adv. Quantum Chem.*, 7, 289 (1973); M. J. Saxton and J. M. Deutch, *J. Chem. Phys.*, 60, 2800 (1974).

$$\Delta\bar{\nu}_{i0}(\text{emission}) = \frac{1}{hc} (2.13 \times 10^{-30}) \left[\sum_{j \neq 0} \left(\frac{1}{\bar{\nu}_{j0}^u} - L_{j0} \right) \frac{f_{j0}^u}{a^3} \frac{n_{j0}^2 - 1}{2n_{j0}^2 + 1} - \sum_{j \neq i} \left(\frac{1}{\bar{\nu}_{ji}^u} - L_{ji} \right) \frac{f_{ji}^u}{a^3} \frac{n_{ji}^2 - 1}{2n_{ji}^2 + 1} \right] + \frac{1}{hc} \frac{(M_{00}^u)^2 - (M_{ii}^u)^2}{a_3} \times \frac{n_0^2 - 1}{2n_0^2 + 1} + \frac{2}{hc} \frac{M_{ii}^u (M_{00}^u - M_{ii}^u)}{a^3} \left[\frac{D-1}{D+2} - \frac{n_0^2 - 1}{n_0^2 + 2} \right] + \frac{2}{hc} \frac{M_{ii}^u (5M_{00}^u - 2M_{ii}^u)}{a^6} (\alpha_0^u - \alpha_i^u) \left[\frac{D-1}{D+2} - \frac{n_0^2 - 1}{n_0^2 + 2} \right]^2 \quad (2)$$

riation and physical meaning of these terms, we define the symbols and briefly consider some of the terms in the above expressions that are pertinent to the experimental results. In eq 1 and 2 the symbols are defined as follows: u represents solute, v represents solvent, 0 indicates the ground state and i, j means the i th and j th excited states, $\bar{\nu}_{ji}^u$ is the energy difference in wavenumbers between the i th and j th excited state of solute molecule, i.e., $\bar{\nu}_{ji}^u hc = E_j - E_i$ (E_j and E_i are the j th and i th excited electronic state energies of the solute molecule respectively), L_{ji} is the weighted mean wave length defined by

$$L_{ji} = \frac{\sum_{a \neq 0} \frac{(M_{a0}^v)^2}{(\bar{\nu}_{a0}^v)^2 - (\bar{\nu}_{ji}^u)^2}}{\sum_{a \neq 0} \frac{\bar{\nu}_{a0}^v (M_{a0}^v)^2}{(\bar{\nu}_{a0}^v)^2 - (\bar{\nu}_{ji}^u)^2}}$$

$\bar{\nu}_{a0}^v$ is the energy difference in wavenumbers between the a th excited and ground state of the solvent molecules, M_{a0}^v is the transition dipole moment of the solvent molecule from the ground state to the a th excited electronic state, n_{ji} is the refractive index of the solvent at frequency $\bar{\nu}_{ji}^u$, n_0 is the refractive index of the solvent at frequency zero, D is the static dielectric constant of the solvent, M_{ii}^u is the permanent dipole moment of the solute molecule in the i th excited state, α_i^u is the isotropic polarizability of the solute molecule in the i th excited state, α_0^u is the isotropic polarizability of the solute molecule in the ground state, and a is the radius of the cavity in which the solute molecule resides.

In the case of a nonpolar solute it is only necessary to consider the first term in these equations which represents the general solvent red shift due to the interaction of induced dipole moments of the solvent molecules with transition dipole moments of the solute. Recall that the relatively small solvent permanent dipole moments seem not to play a prominent role in the gas-to-liquid shifts characterized for benzene. From eq 1 and 2 one obtains

$$\Delta\bar{\nu}_{i0}(\text{absorption}) = \Delta\bar{\nu}_{i0}(\text{emission}) \quad (3)$$

if it can be assumed that the "cavity" radius a does not change for the overall emission/absorption process. However, the results of these experiments clearly point to a difference between the 0-0 absorption and emission features in all solvents studied. In order to explain these results within the context of McRae's theory, one must reconsider the meaning of a and whether or not it should be treated as a constant.

In all cases, the data yield

$$|\Delta\bar{\nu}_{i0}(\text{emission})| > |\Delta\bar{\nu}_{i0}(\text{absorption})|$$

with both shifts negative. All parameters in the first terms

of eq 1 and 2 are the same for emission and absorption. Therefore, a in eq 2 must represent a smaller value than a in eq 1. Physically this means that the transition dipole moments of a solute molecule polarize the surrounding solvent shell and thus the equilibrium benzene/cavity distance for the excited state is smaller than for the ground state. This implies that the excited ${}^1B_{2u}$ /solvent interaction is more attractive than the ${}^1A_{1g}$ /solvent interaction. Thus for emission $a' \approx r_g$ and for absorption $a \approx r_g$.

Assuming that L_{ji} can be represented or approximated by a constant ($L_{ji} = L_0 = 1000 \text{ \AA}$)⁶ and that there exists a linear relation between the factor $(n_{ji}^2 - 1)/(2n_{ji}^2 + 1)$ and the frequencies $\bar{\nu}_{ji}^u$ for different solvents, one may calculate two cavity sizes from the experimental determinations of $\Delta\bar{\nu}_{i0}(\text{absorption})$ and $\Delta\bar{\nu}_{i0}(\text{emission})$. These results are listed in Table III. Since the calculation of a and a' is based on McRae's assumption of a benzene/cyclohexane cavity radius of 3 Å, a and a' values in Table III should be considered as relative values only. Thus, $(a - a')/a$ values should be reasonable even for the non-hydrocarbon solvent NF_3 . In this manner, the relation between gas-to-liquid shifts and polarizability (Figure 6) has been converted into a continuous relation between gas-to-liquid shift and cavity size.

Moreover, the difference between the emission and absorption frequency $\Delta\bar{\nu}_{FC}$ can be seen to be almost entirely due to the ground-state surface (Figure 5). In other words

$$\begin{aligned} \Delta\bar{\nu}_{FC} &\equiv |\Delta\bar{\nu}(\text{emission}) - \Delta\bar{\nu}(\text{absorption})| \\ (E_1 - E_0) &\gg (E_4 - E_3) \\ \Delta\bar{\nu}_{FC}hc &\approx (E_1 - E_0) \end{aligned}$$

It is therefore possible to construct the ground-state repulsive intermolecular potential from the $\Delta\bar{\nu}_{FC}$ values for different solvents and the percentage changes in the intermolecular averaged normal coordinate $(a - a')/a$. This repulsive surface is plotted in Figure 7 along with a quadratic potential for reference. This plot is, of course, based on the assumption that the intermolecular interactions have the same form throughout the C_nH_m series, that is, only cavity size varies to a first approximation from one solvent to another.

The empirical form of the composite normalized (reduced) "surface" is given by $E = 804x^{1.7}$ with x in Å and E in cm^{-1} , based on a value of $a = 3 \text{ \AA}$ and the potential energy normalized to the potential minimum of benzene in cyclohexane.⁶ This surface gives some qualitative measure of the change in energy with intermolecular coordinate in the ground state. The surface is not symmetrical; the attractive part of the potential at $x > r_g$ is likely much less steep. If this potential is folded symmetrically about r_g , however, the value of the force constant is $3.2 \times 10^{-2} \text{ mdyn/\AA}$ and the corresponding harmonic frequency is $8 \times 10^{12} \text{ s}^{-1}$ or $\sim 250 \text{ cm}^{-1}$. These figures give some qualitative measure of what such a potential means in terms of more chemical parameters.

If $r_e > r_g$, the above analysis would predict that absorption features would broaden with increasing temperature. This broadening would then appear on the high-energy side each feature. In such circumstances the emission would change little with temperature. In the discussion of intermolecular potentials in room temperature liquids by Sverdlova et al.,⁷ the increase in molecular size of benzene in the excited ${}^1B_{2u}$ state is interpreted as generating an increase in the repulsive forces only. This eventually leads to a larger value of the intermolecular

(7) O. V. Sverdlova and N. G. Bakhshiev, *Opt. Spectrosc.*, **42**, 163 (1977).

TABLE III: Summary of the First Excited Singlet Transition of C_6D_6 Parameters in Various Solvents^a

	$\Delta\tilde{\nu}_{B_{2u}A_{1g}}(\text{absn})$	$\Delta\tilde{\nu}_{B_{2u}A_{1g}}(\text{emissn})$	$\Delta\tilde{\nu}_{FC}$	n_0	a	a'	$(a - a')/a, \%$
CH_4	-177	-209	32	1.285	3.29	3.11	5.47
C_2H_6	247	305	58	1.377	3.16	2.95	6.64
C_3H_8	270	339	69	1.290	2.87	2.66	7.32
C_2H_4	253	349	96	1.366	3.11	2.79	10.23
C_3H_6	279	398	119	1.357	2.99	2.66	11.03
$1-C_4H_8$	303	427	124	1.396	2.99	2.67	10.81
NF_3	53	61	8	1.188	4.39	4.19	4.55

^a Reported are absorption 0-0 gas-to-liquid shifts ($\Delta\tilde{\nu}_{B_{2u}A_{1g}}(\text{absn})$), emission 0-0 gas-to-liquid shifts ($\Delta\tilde{\nu}_{B_{2u}A_{1g}}(\text{emissn})$), Franck-Condon shifts ($\Delta\tilde{\nu}_{FC} = \Delta\tilde{\nu}_{B_{2u}A_{1g}}(\text{absn}) - \Delta\tilde{\nu}_{B_{2u}A_{1g}}(\text{emissn})$), solvent index of refraction (n_0), ground- and excited-state cavity radius (a and a' , respectively). All calculations are based on $L_0 = 1000$ Å and a benzene/cyclohexane cavity radius of 3.0 Å.⁶ All energies are given in units of cm^{-1} and all distances are given in Å.

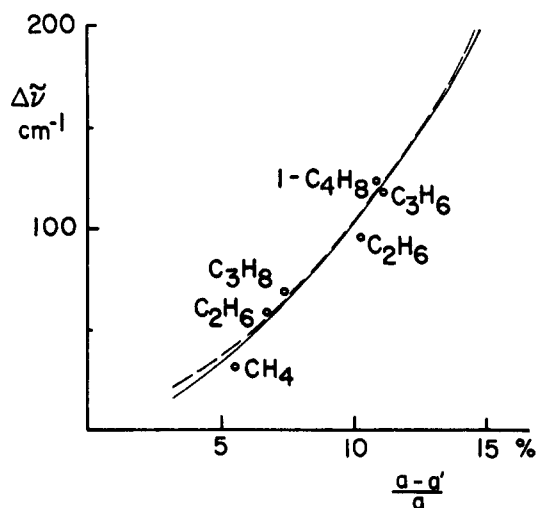


Figure 7. Repulsive intermolecular potential of the benzene/solvent systems. The points (O) represent the projection from equilibrium excited state to the ground-state potential. (—) represents the best fit with the assumed form of $E = \beta x^n$ [$\beta \sim 804$ cm^{-1} and $n \sim 1.7$]. (---) represents the best fit of quadratic form, $E = \beta' x^2$ with $\beta' = 970$ cm^{-1} .

separation ($r_e > r_g$) in their view. Clearly this interpretation is inconsistent with the data presented in this study.

Finally, this calculation of a and a' is based on the limiting case of both solvent and solute molecules with zero permanent dipole moment. In cases for which this is not

a reasonable approach, other terms in eq 1 and 2 would need to be considered. In particular, polar solutes, $n\pi^*$ transitions, and potential hydrogen-bonding situations would render much of our analysis invalid.

Summary and Conclusion

In these experiments dissolved benzene molecules are used to probe the microscopic structure of simple cryogenic molecular liquids. It has been demonstrated that with certain simplifying assumptions, molecular spectra can be used to generate useful information concerning ground- and excited-state intermolecular potential functions. The repulsive potential for the ground-state benzene/hydrocarbon solvent system has been constructed from $\Delta\tilde{\nu}_{FC}$ values for different solvents, since $r_e < r_g$ in this case. Fast intermolecular and intramolecular vibrational relaxation bring the excited state to the equilibrium configuration. Change in the average cavity radius between the ground and excited states is 5–10% in most hydrocarbon solvents studied. The different behavior of absorption and emission features as a function of temperature is explained on the basis of the relative positions of the two intermolecular potential surfaces and the different slopes of these surfaces for repulsive and attractive parts of the potential. This analysis applies to the simplest case of nonpolar solvent and solute and molecules.

Acknowledgment. This work was supported in part by a grant from the National Science Foundation.

Temperature-Dependent Ultraviolet Absorption Spectrum for Dinitrogen Pentoxide

Francis Yao, Ivan Wilson,[†] and Harold Johnston*

Department of Chemistry, University of California, and Materials and Molecular Research Division, Lawrence Berkeley Laboratory, Berkeley, California 94720 (Received: March 12, 1982; In Final Form: May 6, 1982)

The ultraviolet absorption cross sections for N_2O_5 are presented for wavelengths between 200 and 380 nm and for temperatures between 223 and 300 K. The absorption spectrum above 290 nm shows a pronounced temperature dependence.

Introduction

Dinitrogen pentoxide, N_2O_5 , may be a significant reservoir for stratospheric nitrogen oxides, especially at night and in the polar night. The room-temperature ultraviolet cross sections for N_2O_5 were reported between 285 and 380 nm by Jones and Wulf,¹ between 210 and 290 nm by Johnston and Graham,² and between 205 and 310 nm by

Graham.³ This study reinvestigated the absorption cross sections

$$\sigma = (\ln I_0/I)(N_5L)^{-1} \quad (1)$$

where N_5 is the concentration of N_2O_5 in molecules cm^{-3} and L is the optical path in cm, as a function of temper-

[†] Present address: Department of Chemistry, Monash University, Wellington Road, Clayton, Victoria, Australia 3168.

(1) E. L. Jones and O. R. Wulf, *J. Chem. Phys.*, **5**, 873 (1937).
(2) H. S. Johnston and R. A. Graham, *Can. J. Chem.*, **52**, 1415 (1974).
(3) R. A. Graham, Ph.D. Thesis, University of California, Berkeley, 1975.